

2. White, J. G., Southgate, E., Thomson, J. N. & Brenner, S. The structure of the nervous system of the nematode *Caenorhabditis elegans*. *Phil. Trans. R. Soc. Lond. B* **314**, 1–340 (1986).
3. White, J. G., Albertson, D. G. & Anness, M. A. R. Connectivity changes in a class of motoneurons during the development of a nematode. *Nature* **271**, 764–766 (1978).
4. Ambros, V. & Horvitz, H. R. Heterochronic mutants of the nematode *Caenorhabditis elegans*. *Science* **226**, 409–416 (1984).
5. Ambros, V. & Horvitz, H. R. The *lin-14* locus of *Caenorhabditis elegans* controls the time of expression of specific postembryonic developmental events. *Genes Dev.* **1**, 398–414 (1987).
6. Harris, W. A. Neurometamorphosis. *J. Neurobiol.* **21**, 953–957 (1990).
7. Truman, J. Metamorphosis of the central nervous system of *Drosophila*. *J. Neurobiol.* **21**, 1072–1084 (1990).
8. Levine, R. B., Morton, D. B. & Restifo, L. L. Remodeling of the insect nervous system. *Curr. Opin. Neurobiol.* **5**, 28–35 (1995).
9. Alley, K. E. Retrofitting larval neuromuscular circuits in the metamorphosing frog. *J. Neurobiol.* **21**, 1092–1107 (1990).
10. Dotti, C. G. & Banker, G. A. Experimentally induced alterations in the polarity of developing neurons. *Nature* **330**, 254–256 (1987).
11. Chalfie, M., Tu, Y., Euskirchen, G., Ward, W. W. & Prasher, D. C. Green fluorescent protein as a marker for gene expression. *Science* **263**, 802–805 (1994).
12. Nonet, M. L., Saifee, O., Zhao, H., Rand, J. B. & Wei, L. Synaptic transmission deficits in *Caenorhabditis elegans* synaptobrevin mutants. *J. Neurosci.* **18**, 70–80 (1998).
13. Jørgensen, E. M. et al. Defective recycling of synaptic vesicles in synaptotagmin mutants of *Caenorhabditis elegans*. *Nature* **378**, 196–199 (1995).
14. Sulston, J. E. & Horvitz, H. R. Post-embryonic cell lineages of the nematode *Caenorhabditis elegans*. *Dev. Biol.* **56**, 110–156 (1977).
15. Prasher, D. C. & Tsien, R. Y. Wavelength mutations and posttranslational autoxidation of green fluorescent protein. *Proc. Natl Acad. Sci. USA* **91**, 12501–12504 (1994).
16. Ambros, V. & Moss, E. G. Heterochronic genes and the temporal control of *C. elegans* development. *Trends Genet.* **10**, 123–127 (1994).
17. Ruvkun, G. & Giusto, J. The *Caenorhabditis elegans* heterochronic gene *lin-14* encodes a nuclear protein that forms a temporal developmental switch. *Nature* **338**, 313–319 (1989).
18. Euling, S. & Ambros, V. Heterochronic genes control cell cycle progress and developmental competence of *C. elegans* vulval precursor cells. *Cell* **84**, 667–676 (1996).
19. Wightman, B., Bürglin, T. R., Gatto, J., Arasu, P. & Ruvkun, G. Negative regulatory sequences in the *lin-14* 3'-untranslated region are necessary to generate a temporal switch during *Caenorhabditis elegans* development. *Genes Dev.* **5**, 1813–1824 (1991).
20. Wightman, B., Ha, I. & Ruvkun, G. Post-transcriptional regulation of the heterochronic gene *lin-14* by *lin-4* mediates temporal pattern formation in *C. elegans*. *Cell* **75**, 855–862 (1993).
21. Purves, D. & Hadley, R. D. Changes in the dendritic branching of adult mammalian neurones revealed by repeated imaging *in situ*. *Nature* **315**, 404–406 (1985).
22. Purves, D. & Lichtman, J. W. Elimination of synapses in the developing nervous system. *Science* **210**, 153–157 (1994).
23. Wigston, D. J. Repeated *in vivo* visualization of neuromuscular junctions in adult mouse lateral gastrocnemius. *J. Neurosci.* **10**, 1753–1761 (1990).
24. Chen, L., Folsom, D. B. & Ko, C.-P. The remodelling of synaptic extracellular matrix and its dynamic relationship with nerve terminals at living frog neuromuscular junctions. *J. Neurosci.* **11**, 2920–2930 (1991).
25. Bailey, C. H. & Kandel, E. R. Structural changes accompanying memory storage. *Annu. Rev. Physiol.* **55**, 397–426 (1993).
26. Goodman, C. S. & Shatz, C. J. Developmental mechanisms that generate precise patterns of neuronal connectivity. *Cell* **72**, 77–98 (1993).
27. Brenner, S. The genetics of *Caenorhabditis elegans*. *Genetics* **77**, 71–94 (1974).
28. Clark, S. G., Lu, X.-W. & Horvitz, H. R. The *Caenorhabditis elegans* locus *lin-15*, a negative regulator of a tyrosine kinase signaling pathway, encodes two different proteins. *Genetics* **137**, 987–997 (1994).
29. Naito, M., Kohara, Y. & Kurosawa, Y. Identification of a homeobox-containing gene located between *lin-45* and *unc-24* on chromosome IV in the nematode *Caenorhabditis elegans*. *Nucleic Acids Res.* **20**, 2967–2969 (1992).

Acknowledgements. We thank M. Nonet for the SNB-GFP DNA; V. Ambros and Y. Hong for *lin-14* alleles and *lin-14(+)* genomic DNA; G. Ruvkun, B. Reinhart and F. Slack for anti-LIN-14 antibodies; and A. Chisholm, A. Zahler, J. Sisson, V. Ambros, M. Nonet, M. Zhen, I. Chin-Sang and members of the Jin and Chisholm labs for helpful discussions and comments. Some strains used in this work were provided by the *Caenorhabditis* Genetics Center, which is funded by the NIH Center for Research Resources. S.J.H. was supported by a Predoctoral GAANN fellowship. Y.J. is an Alfred P. Sloan Research Fellow.

Correspondence and requests for materials should be addressed to Y.J. (e-mail: jin@biology.ucsc.edu).

Three-dimensional segregation of supramolecular activation clusters in T cells

Colin R. F. Monks*, Benjamin A. Freiberg*†, Hannah Kupfer*, Noah Siciak* & Abraham Kupfer*†‡

* Division of Basic Science, Department of Pediatrics, National Jewish Medical and Research Center, 1400 Jackson Street, Denver, Colorado 80206, USA
 † Departments of † Immunology and ‡ Cellular and Structural Biology, University of Colorado Health Sciences Center, Denver, Colorado 80262, USA

Activation of T cells by antigen-presenting cells (APCs) depends on the complex integration of signals that are delivered by multiple antigen receptors. Most receptor-proximal activation events in T cells^{1,2} were identified using multivalent anti-receptor antibodies, eliminating the need to use the more complex APCs.

As the physiological membrane-associated ligands on the APC and the activating antibodies probably trigger the same biochemical pathways, it is unknown why the antibodies, even at saturating concentrations, fail to trigger some of the physiological T-cell responses³. Here we study, at the level of the single cell, the responses of T cells to native ligands. We used a digital imaging system and analysed the three-dimensional distribution of receptors and intracellular proteins that cluster at the contacts between T cells and APCs during antigen-specific interactions^{3,4}. Surprisingly, instead of showing uniform oligomerization, these proteins clustered into segregated three-dimensional domains within the cell contacts. The antigen-specific formation of these new, spatially segregated supramolecular activation clusters may generate appropriate physiological responses and may explain the high sensitivity of the T cells to antigen.

Engaged and activated lymphocyte-bound receptors, together with their associated proteins, can be identified and studied, at the single-cell level, by their localized clustering at the T-cell-APC contact^{3–6}. Cloned D10 T cells, specific for the antigens conalbumin and IAK, were mixed with APCs that had been pulsed with conalbumin (500 µg ml⁻¹), and, 30 min later, the cell mixtures were fixed and doubly immunofluorescently labelled with antibodies specific for talin and for protein kinase C (PKC)-θ (Fig. 1). Sets of 46 serial optical sections, 0.2 µm apart along the z axis, were recorded for each of the immunofluorescent labels. The three-dimensional image sets, which span the entire boundaries of the cell conjugates, were computationally processed using deconvolution software to eliminate the out-of-focus haze, thereby improving the spatial resolution and fidelity of the data⁷.

Figure 1a, b shows the labelling for talin and PKC-θ in one of the deconvolved optical sections, through the middle of the cell conjugate. Such single two-dimensional images show that both talin and PKC-θ clustered at the cell contact, as reported previously^{3,8}, but they also indicated some differential localization. Surprisingly, the reconstructed three-dimensional views of the cell contacts showed that these proteins were present in two distinct, non-overlapping domains (Fig. 1d, e). Talin was enriched in most of the contact area, but was absent from a smaller central region (Fig. 1d). In contrast, PKC-θ was enriched in only a small contact area (Fig. 1e) from which talin was largely excluded (Fig. 1f). The same contact domains were also seen when other anti-talin and PKC-θ antibodies

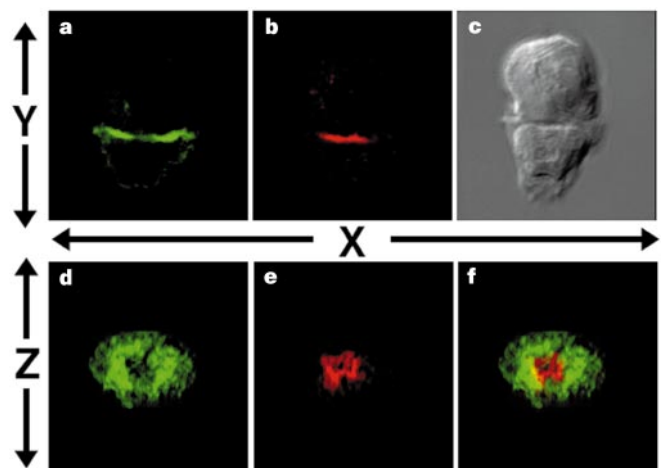


Figure 1 The localization of talin and PKC-θ at the three-dimensionally reconstructed T-cell-APC contact site. The antigen-specific D10-CH12 cell conjugates were labelled with guinea-pig antibodies specific for talin (a, d) and rabbit antibodies specific for PKC-θ (b, e). a, b, A single 2D optical section (along the x-y axis) in the centre of the cell conjugate whose Nomarski image is shown in c. d-f, The 3D view of the entire cell contact (along the x-z axis). f, Both talin (green) and PKC-θ (red) are shown at the cell contact. Note that the two proteins are present in two distinct domains.

were used and when the fluorescent labels for talin and PKC- θ were switched (data not shown). Moreover, similar three-dimensional contact domains were seen in control experiments in which the T-cell-APC conjugates were labelled singly with either anti-talin or anti-PKC- θ antibodies (data not shown). None of these domains were seen in antigen-nonspecific conjugates, for which neither talin nor PKC- θ was enriched in the contacts.

The activation-induced segregation of talin and PKC- θ indicated that the molecular composition of the cytoplasmic side of the contact is not uniform. To determine whether clustered receptors also spatially segregate in the T-cell-APC contact sites, we analysed the three-dimensional distribution of two receptors, LFA-1 and the T-cell antigen receptor (TCR). LFA-1 associates with talin, but not with PKC- θ , in activated T cells^{3,4,9}. Activation of the TCR by the APC is required for the translocation of both PKC- θ and talin,

but antibody co-capping experiments failed to show an association between the TCR and either talin or PKC- θ ^{3,4,9}. We conjugated T cells from AD10-TCR transgenic mice with CH12 cells, which had been pulsed with the antigen pigeon cytochrome C (PCC) ($50 \mu\text{g ml}^{-1}$). The cell mixtures were doubly labelled with anti-LFA1 and either anti-talin or anti-PKC- θ antibodies (Fig. 2). The immunofluorescent images show that LFA-1, talin and PKC- θ cluster at the cell contact in antigen-specific conjugates (Fig. 2b, c, h, i) but not in antigen-nonspecific conjugates (Fig. 2n, o). The three-dimensional reconstructed views of the cell contacts showed that LFA-1 and talin were enriched in most of the contact, and both were excluded from the same central contact area (Fig. 2d-f). In contrast, LFA-1 and PKC- θ were segregated into two different contact domains (Fig. 2j-l).

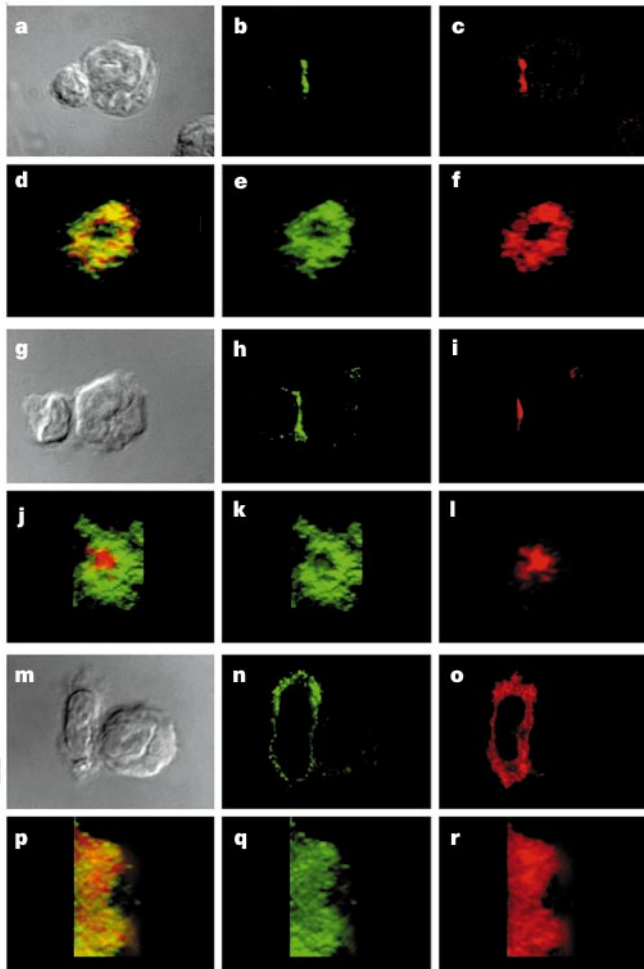


Figure 2 The 3D redistribution of LFA-1 in antigen-specific T-APC conjugates. In Figs 2, 3, 5, 7 and 8, each cell conjugate is shown in two rows of three panels. The top row of each pair of rows starts with a Nomarski image. The next two panels show each of the two labels in a single optical section along the x - y axis. The bottom row of each pair starts with a panel showing both labels in the 3D view of the entire contact area (x - z axis). The next two panels show each of the corresponding labels in the 3D view of the contact. The 3D views were magnified by 50% to show more detail. Antigen-specific (a-l) and antigen-nonspecific (m-r) conjugates of AD10-CH12 cells are shown. The cells were labelled with rat antibodies specific for LFA-1 (in green, b, e, h, k, n, q), guinea-pig antibodies against talin (in red, c, f, o, r) or rabbit antibodies specific for PKC- θ (in red, i, l). Note that LFA-1 is enriched in most of the contact, like talin, but is excluded from PKC- θ . None of these proteins cluster and organize in the antigen-nonspecific conjugates.

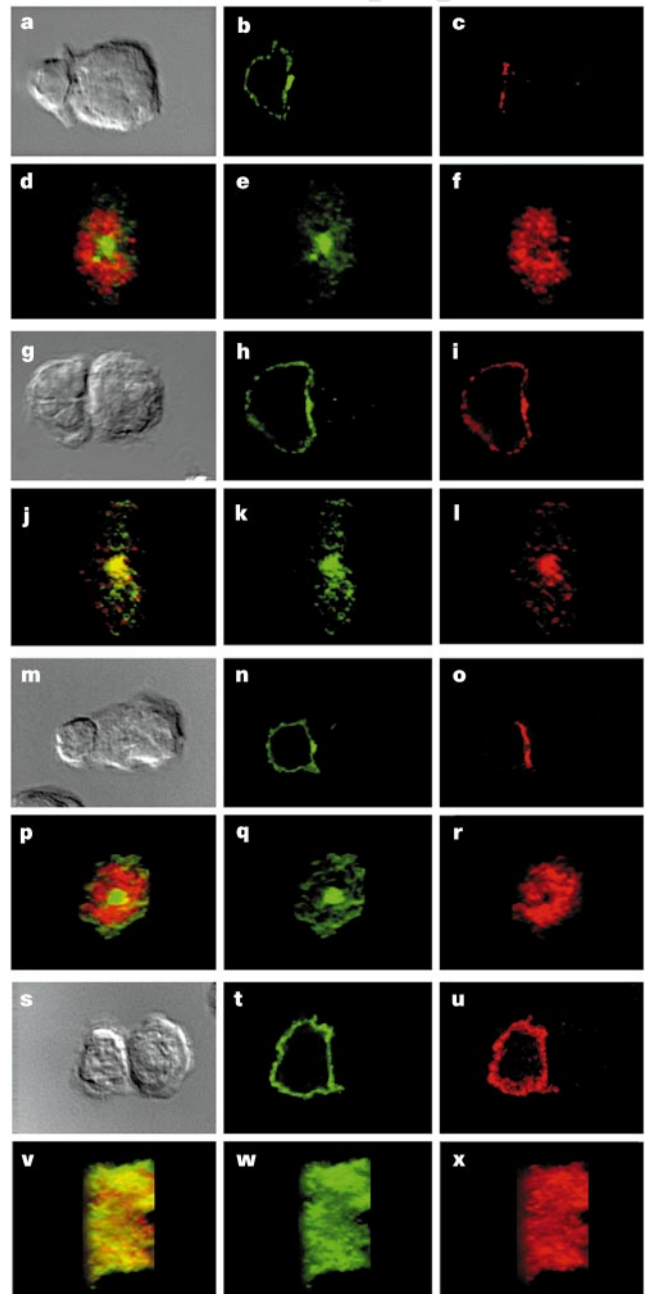


Figure 3 The 3D redistribution of TCR-CD3 in antigen-specific (a-r) but not in antigen-nonspecific (s-x) T-cell-APC conjugates. D10-CH12 (a-l) and AD10-CH12 (m-x) cell conjugates were labelled with anti-CD3 antibodies (in green, b, e, h, k, n, q, t, w) and any of the following antibodies (in red): anti-LFA1 (c, f), anti-V β 8 chain of the TCR (i, l) or anti-talin (o, r, u, x). See Fig. 2 legend for layout of panels.

The formation of these three-dimensional domains depended on recognition of specific antigen. In antigen-nonspecific conjugates, LFA-1 and talin remained randomly distributed (Fig. 2p–r).

We determined the spatial distribution of the TCR–CD3 complex in antigen-specific AD10–CH12 and D10–CH12 cell conjugates (Fig. 3). Clusters of CD3 and LFA-1 were observed in the contact area (Fig. 3a–f). There were, however, significant quantitative and qualitative differences between the clusters of LFA-1 and CD3. Quantitative three-dimensional analysis of the entire cell membranes showed that $78 \pm 9\%$ (mean \pm s.d.) ($n = 20$) of total surface LFA-1 was present at the cell contacts, and only $42 \pm 9\%$ ($n = 20$) of the TCR was in the contact (Fig. 4a). The fraction of the TCR in the contact was only slightly higher than that of the class I major histocompatibility complex (MHC) protein H2k, a membrane protein that did not cluster ($36 \pm 5\%$; $n = 10$) (Figs 4a and 5o, r). The contact may contain both ligand-bound and unbound receptors. Receptor ligation at the cell contact results in a localized enrichment that is proportional to the extent of binding^{4,6,10}. We determined the fraction of clustered (that is, bound) LFA-1 and TCR by quantifying contact voxels whose intensity was higher than the intensity of the voxels in the rest of the T-cell membrane. In this analysis, only a small fraction of total TCR ($6 \pm 3\%$) appeared to be ligand-bound in the contact. In contrast, most LFA-1 ($78 \pm 9\%$) appeared to be ligand-bound (Fig. 4b). This difference concurred with the expected relative concentrations of the cell-adhesion molecule ICAM and specific peptide–IAk (IAk is a class II MHC protein) complexes¹¹, the ligands for the LFA-1 and TCR, respectively. In addition, although clustered LFA-1 was present along most of the contact area, the clustered TCR was confined to only $6.2 \pm 2.4\%$ of the contact area. To estimate the frequency of TCR clustering among all T-cell–APC couples, we used Nomarski optics to identify cell conjugates and blindly imaged their TCR labelling. Clustered TCR was detected in 28 of such 29 randomly selected cell conjugates.

Three-dimensional analysis of the cell contacts showed that clustered LFA-1 and TCR were spatially segregated from each other (Fig. 3d–f). Similar three-dimensional domains were seen in control experiments in which the cells were either singly labelled for only one of the receptors or doubly labelled with other antibody combinations. These results indicate that the mutual exclusion of the two receptors reflected their distinct spatial distribution and was

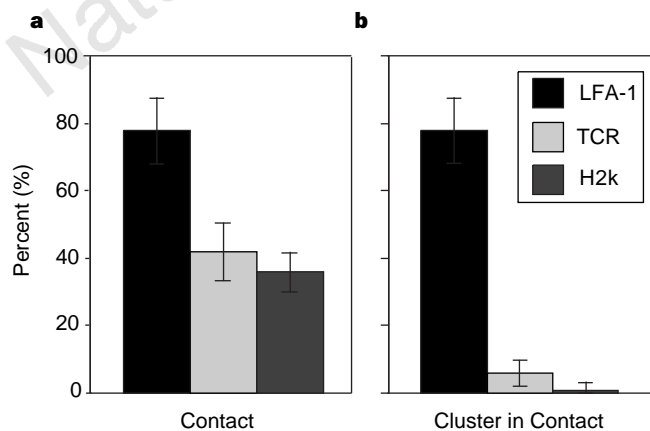


Figure 4 Quantitative analysis of the fractional distribution of receptors for the T-cell–APC contact site. Conjugates of D10 and CH12 cells, which were pulsed with $500 \mu\text{g ml}^{-1}$ conalbumin, were singly labelled with anti-LFA1, anti-V β 8 chain of the TCR or anti-H2k antibodies. 3D images of cell couples were recorded and the localized surface expression of the different receptors was quantified. **a**, The labelling in the entire cell contact expressed as a percentage of total T-cell labelling. **b**, The clustered (that is, engaged) receptors at the contact as a percentage of total T-cell labelling.

not due to an inability to label two antibodies in the same domain. The clustering of the TCR was further confirmed by doubly labelling D10–CH12 cells with antibodies directed against CD3– ϵ and V β 8–TCR (Fig. 3g–l), as well as by labelling the cytoplasmic tail of the ζ -chain of CD3 (not shown). The spatial segregation of the clustered TCR was detected in several different antigen-specific T-cell clones (as in Fig. 3) and, significantly, in *ex vivo* T cells from TCR-transgenic mice (Fig. 3a–f). The TCR did not cluster and did not form a centrally focused domain in antigen-nonspecific conjugates of T-helper (T_H) cells and APCs (Fig. 3t, v, w).

In extra control experiments, AD10–CH12 conjugates were doubly labelled with anti-CD3 antibodies and with a murine antibody specific for H2k (Fig. 5m–r). H2k is a membrane glycoprotein that is not expected to be involved in this interaction, as the TCRs of the AD10 T cells recognize peptide that is bound to class II, not class I, MHC. Although the TCR–CD3 was focused in the contact (Fig. 5n, p, q) the labelling for H2k remained uniform and was neither enriched nor depleted from any domain (Fig. 5o, p, r). These results indicate that the segregation of membrane proteins into contact domains is a specific and regulated process, and is not caused by the passive sorting of proteins. Thus, the three-dimensional analysis of the entire site of interaction between T_H cells and APCs shows, surprisingly, that receptors and intracellular proteins that are

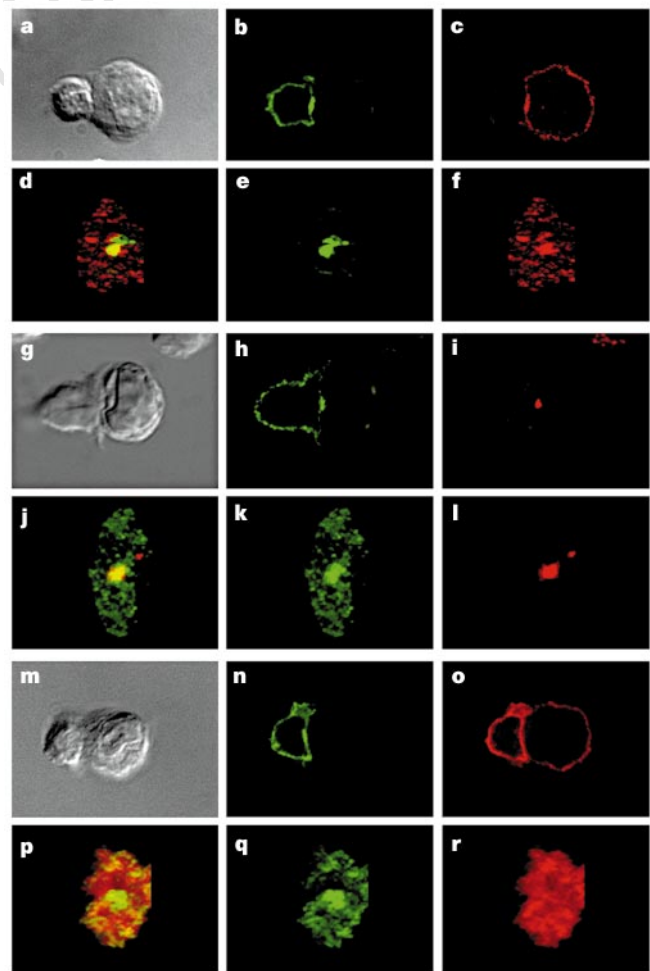


Figure 5 The 3D redistribution of TCR–CD3 and class II MHC in antigen-specific T-cell–APC conjugates. AD10–CH12 (**a–f** and **m–r**) and D10–CH12 (**g–l**) conjugates were labelled with anti-CD3 antibody (in green, **b, e, h, k, n, q**) and with one of the following antibodies (in red): anti-IEk (**c, f**), anti-IA α (**i, l**) and anti-H2k (**o, r**). Note that class II antigens co-cluster with the TCR but that class I antigens do not co-cluster. See Fig. 2 legend for panel layout.

involved in physiological T-cell activation are organized into distinct spatial domains. We name these three-dimensional contact domains 'supramolecular activation clusters' (SMACs), which include the peripheral SMAC (p-SMAC) and the central TCR-SMAC (c-SMAC) (Fig. 6).

Because the SMACs are seen only in antigen-specific conjugates, it is likely that the c-SMAC is the site of TCR ligation. To further test this idea, we determined whether class II MHC, TCR ligand, clusters in the APC, mirroring the c-SMAC in the T cell. As the CH12 cells express both IAk and IEk class II MHC, we used AD10 T cells that recognize PCC peptide bound to IEk and D10 T cells that recognize conalbumin peptide bound to IAk. 14-4-4, a murine monoclonal antibody specific for IEk, and a rabbit antibody directed against the cytoplasmic tail of IA- α (ref. 12) were used to selectively localize IEk and IAk, respectively. Clustering of surface IEk (Fig. 5c) was detected at the contact of AD10-CH12 conjugates that were doubly labelled with anti-CD3 and anti-IEk antibodies (Fig. 5a-f). Remarkably, the clustered IEk on the APC mirrored the c-SMACs on the T cell (Fig. 5d-f). Unlike IEk, labelled IAk was not clustered at the AD10-CH12 contact area (results not shown). The reverse results were seen in D10-CH12 cells. In these conjugates, IAk, but not IEk, was clustered on the CH12 cells (Fig. 5g-l). Again, the IAk cluster mirrored the c-SMAC, indicating that the clustered TCR-CD3 complexes at the c-SMAC are probably bound to their ligands.

To determine whether the SMACs are important for T-cell activation, CH12 cells were treated with CA37 ($5 \mu\text{g ml}^{-1}$), an agonist peptide, or with either E8A or E8T ($5 \mu\text{g ml}^{-1}$), which are altered peptides containing a single amino-acid substitution at position 8 (ref. 13). Although the agonist peptide causes extensive T-cell proliferation and cytokine production, the altered peptides function as antagonist peptides for T cells derived from D10-TCR transgenic mice and do not trigger cytokine production or T-cell proliferation (for a complete description of these peptides, see ref. 13). The T-cell-APC conjugates were doubly labelled with anti-

CD3 antibody, to detect the c-SMAC, and anti-talin antibody, to visualize p-SMAC (Fig. 7). In the agonist-induced cell conjugates, both talin and CD3 clustered at the cell contact and both p- and c-SMACs were formed (Fig. 7a-f). Talin and CD3 also clustered at the cell contacts in the altered-peptide-induced conjugates (Fig. 7h, i), indicating that the TCR was engaged and that activation signals for talin translocation were delivered. This is in agreement with previous studies showing that activation of talin clustering can be

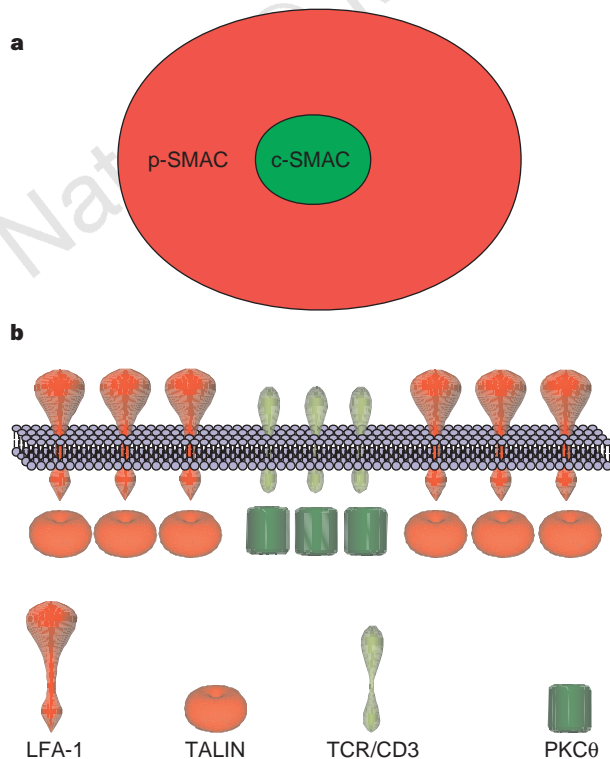


Figure 6 The p-SMAC and c-SMAC. **a**, 3D view of the entire cell contact. **b**, Cross-section through the centre of a T-cell-APC contact, showing the molecular clustering and segregation of the TCR, LFA-1, PKC- θ and talin.

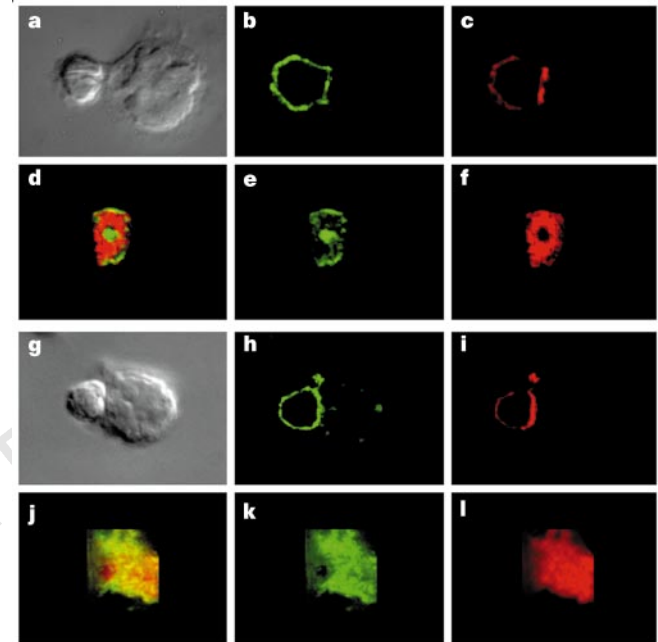


Figure 7 Agonist peptides and not altered peptides cause the formation of SMACs. Cell conjugates containing T cells from D10-TCR transgenic mice and CH12 cells that were pulsed with either CA37, an agonist peptide (**a-f**), or E8A, an antagonistic peptide (**g-l**), were labelled with anti-CD3 antibody (in green, **b, e, h, k**) and anti-talin antibody (in red, **c, f, i, l**). See Fig. 2 legend for panel layout.

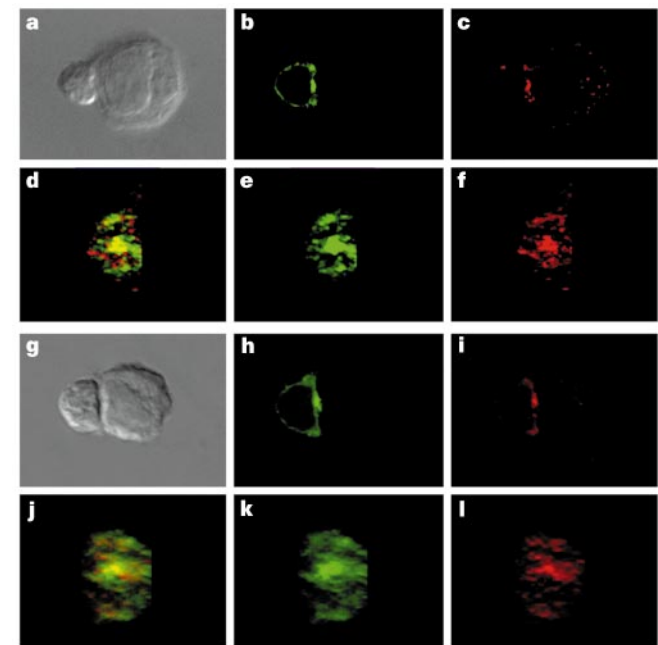


Figure 8 The rapid translocation of Fyn and Lck to c-SMACs. AD10-CH12 cell conjugates were fixed 5 (for Lck) or 13 (for Fyn) min after cell conjugation and labelled with anti-CD3 (in green, **b, e, h, k**), anti-Fyn (in red, **c, f**) or anti-Lck (in red, **i, l**) antibodies. See Fig. 2 legend for panel layout.

functionally uncoupled from the induction of T-cell proliferation^{3,8}. Importantly, in these conjugates the clustered CD3 and talin failed to segregate into SMACs and remained unorganized throughout the contact (Fig. 7j–l). The SMACs failed to form even when the CH12 cells were pulsed with higher concentrations of E8A (up to 50 $\mu\text{g ml}^{-1}$). These results indicate that receptor engagement by itself, although necessary, is not sufficient to form the SMACs and that receptor ligation without the formation of SMACs is not sufficient to properly activate the T cells.

The formation of SMACs may explain several important issues related to the physiological activation of T cells. The TCR–CD3 complexes do not remain randomly dispersed after binding ligand. Instead, they immediately begin to assemble into a c-SMAC (Fig. 8). Three-dimensional analysis indicated that, as early as 5–13 min after cell conjugation, the Src-family kinases Lck and Fyn were also enriched in the c-SMAC (Fig. 8). Other signalling proteins at the p-SMAC (A.K. *et al.*, manuscript in preparation) indicate that the p-SMAC may also act in T-cell signalling, albeit providing signals that differ from the c-SMAC signals. It is thus likely that the regulated segregation of activated receptors and their associated proteins would generate unique signals that would not be otherwise generated by randomly co-aggregated receptors.

Activation of receptor-associated tyrosine kinases and the appropriate tyrosine phosphorylation of the cytoplasmic tails of receptors and of multiple intracellular proteins^{1,2} requires the formation of receptor signalling complexes^{14–16}. The SMACs identify a new, additional level of regulated molecular interactions, whereby individual receptor signalling complexes appear to interact with each other to form distinct supramolecular complexes. Although the mechanisms that generate the SMACs are still unknown, it is likely that the SMACs are assembled by receptor interactions with extracellular ligands and with intracellular signalling and linking proteins, which can express multiple protein-interaction domains^{14–16}. We are now studying the mechanisms that regulate the formation of the SMACs and their roles in determining the fate of the activated T cells. □

Methods

The T and B cells, the formation of cell conjugates, the antibodies and the immunofluorescence labelling have been described^{3,7}. The agonist peptide CA37 and the altered peptides E8A and E8T, containing a substitution of the glutamic acid at position 8 with alanine or threonine, as well as all the D10-related cells, have been described¹³ and were a gift from C. A. Janeway. The anti-I α antibody was a gift from J. Miller. P. Marrack provided the AD10–TCR transgenic mice. The three-dimensional immunofluorescence and the corresponding Nomarski images of the cells were recorded by a digital fluorescence microscopy system (Intelligent Imaging Innovations, Denver, CO). The imaging system included a chilled charge-coupled device (CCD) slow-scan camera (Orbis, SpectraSource, Westlake Village, CA), a Zeiss Axiophot microscope, a z-axis stepper motor (Della, Estes Park, CO), and excitation and emission filter wheels (LEP, Hawthorne, NY) with narrow-band optical filters (Chromatech, Brattleboro, VT). All of these components were controlled by SlideBook software (Intelligent Imaging Innovations). SlideBook software was used for three-dimensional image capture, deconvolution and rendering. At least 100 cell conjugates per coverslip were analysed. All the three-dimensional image sets were analysed using Nearest Neighbour Deconvolution. In addition, at least 25 of the same conjugates were also processed by the much slower Constrained Iterative Deconvolution, applying 20 iterations on the three-dimensional image sets. Additional iterations had no detectable effects on the images. There were no obvious differences between the images that were generated with the two different deconvolutions. The three-dimensional front views of the cell contacts were generated as orthographic projections of the voxels that make up the T-cell–APC contact.

Received 23 June; accepted 4 August 1998.

- Weiss, A. & Littman, D. R. Signal transduction by lymphocyte antigen receptors. *Cell* **76**, 263–274 (1994).
- Qian, D. & Weiss, A. T cell antigen receptor signal transduction. *Curr. Opin. Cell Biol.* **9**, 205–212 (1997).

- Monks, C. R., Kupfer, H., Tamir, I., Barlow, A. & Kupfer, A. Selective modulation of protein kinase C- θ during T-cell activation. *Nature* **385**, 83–86 (1997).
- Podack, E. R. & Kupfer, A. T-cell effector functions: mechanisms for delivery of cytotoxicity and help. *Annu. Rev. Cell Biol.* **7**, 479–504 (1991).
- Singer, S. J. Intercellular communication and cell-cell adhesion. *Science* **255**, 1671–1677 (1992).
- Kupfer, A. & Singer, S. J. Cell biology of cytotoxic and helper T cell functions: immunofluorescence microscopic studies of single cells and cell couples. *Annu. Rev. Immunol.* **7**, 309–337 (1989).
- Hiraoka, Y., Sedat, J. W. & Agard, D. A. Determination of three-dimensional imaging properties of a light microscope system. Partial confocal behavior in epifluorescence microscopy. *Biophys. J.* **57**, 325–333 (1990).
- Kupfer, A. & Singer, S. J. The specific interaction of helper T cells and antigen-presenting B cells. IV. Membrane and cytoskeletal reorganizations in the bound T cell as a function of antigen dose. *J. Exp. Med.* **170**, 1697–1713 (1989).
- Kupfer, A., Burn, P. & Singer, S. J. The PMA-induced specific association of LFA-1 and talin in intact cloned T helper cells. *J. Mol. Cell. Immunol.* **4**, 317–325 (1990).
- McCloskey, M. A. & Poo, M. M. Contact-induced redistribution of specific membrane components: local accumulation and development of adhesion. *J. Cell Biol.* **102**, 2185–2196 (1986).
- Harding, C. V. & Unanue, E. R. Quantitation of antigen-presenting cell MHC class II/peptide complexes necessary for T-cell stimulation. *Nature* **346**, 574–576 (1990).
- Anderson, M. S., Swier, K., Arneson, L. & Miller, J. Enhanced antigen presentation in the absence of the invariant chain endosomal localization signal. *J. Exp. Med.* **178**, 1959–1969 (1993).
- Dittel, B. N., Sant'Angelo, D. B. & Janeway, C. A. Jr Peptide antagonists inhibit proliferation and the production of IL-4 and/or IFN- γ in T helper 1, T helper 2, and T helper 0 clones bearing the same TCR. *J. Immunol.* **158**, 4065–4073 (1997).
- Schlessinger, J. SH2/SH3 signaling proteins. *Curr. Opin. Genet. Dev.* **4**, 25–30 (1994).
- Lemmon, M. A., Ferguson, K. M. & Schlessinger, J. PH domains: diverse sequences with a common fold recruit signaling molecules to the cell surface. *Cell* **85**, 621–624 (1996).
- Pawson, T. & Scott, J. D. Signaling through scaffold, anchoring, and adaptor proteins. *Science* **278**, 2075–2080 (1997).
- Kupfer, H., Monks, C. R. & Kupfer, A. Small splenic B cells that bind to antigen-specific T helper (Th) cells and face the site of cytokine production in the Th cells selectively proliferate: immunofluorescence microscopic studies of Th–B-antigen presenting cell interactions. *J. Exp. Med.* **179**, 1507–1515 (1994).

Acknowledgements. We thank C. A. Janeway Jr, J. Miller and P. Marrack for reagents, cell lines and transgenic mice; J. Kappler and P. Marrack for comments; and D. Littman and J. Schlessinger for advice and critical reading of this manuscript. These studies were supported in part by grants from the NIH.

Correspondence and requests for materials should be addressed to A.K.

Yeast G1 cyclins are unstable in G1 phase

Brandt L. Schneider*[†], E. Elizabeth Patton*[‡], Stefan Lanker[§], Michael D. Mendenhall[¶], Curt Wittenberg[§], Bruce Futcher[†] & Mike Tyers[‡]

[†] Cold Spring Harbor Laboratory, PO Box 100, Cold Spring Harbor, New York 11724, USA

[‡] Programme in Molecular Biology and Cancer, Samuel Lunenfeld Research Institute, Mount Sinai Hospital, 600 University Avenue, Toronto, Canada M5G 1X5, and Graduate Department of Molecular and Medical Genetics, University of Toronto, 1 Kings College Circle, Toronto, Canada M5S 1A8

[§] Department of Molecular Biology, The Scripps Research Institute, 10550 North Torrey Pines Road, La Jolla, California 92037, USA

[¶] Markey Cancer Center, Dept. of Biochemistry, University of Kentucky, Lexington, KY 40536-0096, USA

* These authors contributed equally to this work.

In most eukaryotes, commitment to cell division occurs in late G1 phase at an event called Start in the yeast *Saccharomyces cerevisiae*¹, and called the restriction point in mammalian cells². Start is triggered by the cyclin-dependent kinase Cdc28 and three rate-limiting activators, the G1 cyclins Cln1, Cln2 and Cln3 (ref. 3). Cyclin accumulation in G1 is driven in part by the cell-cycle-regulated transcription of *CLN1* and *CLN2*, which peaks at Start². *CLN* transcription is modulated by physiological signals that regulate G1 progression^{4,5}, but it is unclear whether Cln protein stability is cell-cycle-regulated. It has been suggested that once cells pass Start, Cln proteolysis is triggered by the mitotic cyclins Clb1, 2, 3 and 4 (ref. 6). But here we show that G1 cyclins are unstable in G1 phase, and that Clb–Cdc28 activity is not needed for G1 cyclin turnover. Cln instability thus provides a means to couple Cln–Cdc28 activity to transcriptional regulation and protein synthetic rate in pre-Start G1 cells.

^{||} Present address: Department of Molecular and Medical Genetics, School of Medicine, Oregon Health Sciences University, 3181 SW Sam Jackson Park Road, Portland, Oregon 97201-3098, USA.